Structure−Property Relationship in *py*-Hexahydrocinchonidine Diastereomers: Ab Initio and NMR Study

György Szöllösi,*,†,‡ Abhijit Chatterjee,† Péter Forgó,§ Mihály Bartók,‡,§ and Fujio Mizukami†

Laboratory for Membrane Chemistry, National Institute of Advanced Industrial Science and Technology, AIST Tohoku, 4-2-1, Nigatake, Miyagino-ku, Sendai, 983-8551, Japan, and Organic Catalysis Research Group of the Hungarian Academy of Sciences and Department of Organic Chemistry, University of Szeged, H-6720, Dóm tér 8, Szeged, Hungary

Received: September 12, 2004; In Final Form: November 15, 2004

Two *py*-hexahydrocinchonidine diastereomers were selectively obtained in the heterogeneous catalytic hydrogenation of cinchonidine over supported Pt catalyst. The two isolated compounds when used as chiral base catalysts in the Michael addition of a β-keto ester to methyl vinyl ketone gave products of opposite configuration in excess. To trace the reason of this behavior, in the present study, the structures of the two diastereomers were fully optimized by ab initio quantum chemical calculation. These results were then compared with several nuclear Overhauser enhancement spectroscopy (NOESY) signal intensities from the spectra of the two compounds. Further we performed a conformational search on all the optimized geometries independently for the two flexible torsional angles, which are linking the quinuclidine and tetrahydroquinoline moieties present in these molecules. This study allowed us to propose the configuration of the $C_{4'}$ chiral center. Thus, the product mixture resulted in the hydrogenation of cinchonidine containing the 4′-(*S*)-diastereomer in excess (de = 20%). According to the computation results the 4′-(*S*)-diastereomer is more stable than the 4′-(*R*)-diastereomer. The 4′-(*S*)-conformer obtained by computation has lower electronic energy than the structures obtained for the 4′-(*R*)-diastereomer, which may explain the excess formation of the first one. The results of the Michael addition catalyzed by these diastereomers were interpreted on the basis of these conclusions.

1. Introduction

In the production of enantiomerically pure products, cinchona alkaloids are among the most often used natural chiral compounds.[1,2] They had been successfully used in several asymmetric syntheses as chiral auxiliaries or catalysts.[3] Derivatives of the natural cinchona alkaloids often provided higher enantioselectivities compared to that achieved by the use of the parent compounds.[4−9] Systematic variation of their structures was used in the elucidation of the role of different moieties or functional groups of the alkaloid molecules and constituted valuable information in the design of efficient synthetic chiral catalysts.[4,10−18] The natural cinchona alkaloids can be hydrogenated over heterogeneous metal catalysts. Under mild conditions they are transformed in dihydro derivatives by hydrogenation of their vinyl group. The use of higher H_2 pressures and/or elevated temperatures leads to the formation of hexa- and/or dodecahydro derivatives by partial or total hydrogenation of the quinoline moiety. The preparation of these derivatives of some cinchona alkaloids has been described.[19−22] They have been tested as modifiers in the enantioselective heterogeneous catalytic hydrogenation of α-keto esters,[10,11,14] a reaction reported first by Orito et al.[23,24] The presence of hydrogenated cinchona derivatives in the liquid phase during this reaction showed that the modifier may also be hydrogenated, leading to a decrease in the ee.[25,26]

Recently, we have reported the preparation of hexahydrocinchonine and cinchonidine derivatives by hydrogenation over Pt/Al_2O_3 catalyst.[27] The isolated compounds have been used as chiral modifiers in the heterogeneous hydrogenation of ethyl pyruvate and as chiral base catalysts in the Michael addition of ethyl 2-oxocyclopentanecarboxylate (ECP) to methyl vinyl ketone (MVK). In the latter reaction the two hexahydrocinchonidine isomers gave products of opposite configuration in excess. The interpretation of these surprising results was hindered by the lack of knowledge of the configuration of the $C_{4'}$ chiral center and of the conformational behavior of these compounds.

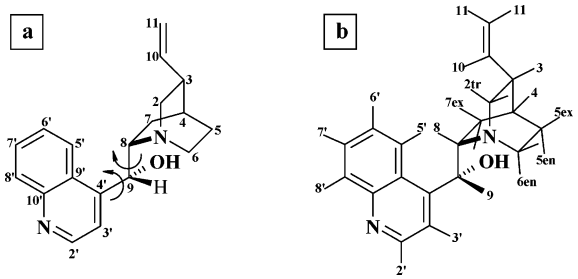

Figure 1. Cinchonidine (CD) atom labeling: (a) C atoms; (b) H atoms.

Cinchona alkaloids have a remarkably high conformational freedom. Rotation around the $C_{4'}-C_9$ and C_9-C_8 bonds (see Figure 1a) may lead to conformers of similar energies. The conformers may favor the formation of different products in excess.[28] As a consequence, to elucidate the reaction mechanism on a molecular level, investigation of the conformational behavior of these cinchona derivatives is necessary. Several theoretical investigations on the conformational behavior of natural cinchona alkaloids and some of their derivatives using semiempirical and ab initio methods have been published.[29−34]

* Corresponding author. Phone/Fax: (+36) 62-544-200. E-mail: szollosi@chem.u-szeged.hu.

† National Institute of Advanced Industrial Science and Technology.

‡ Organic Catalysis Research Group of the Hungarian Academy of Sciences and the Department of Organic Chemistry, University of Szeged.

§ Department of Organic Chemistry, University of Szeged.

10.1021/jp045882t CCC: $30.25
Published on Web 01/15/2005

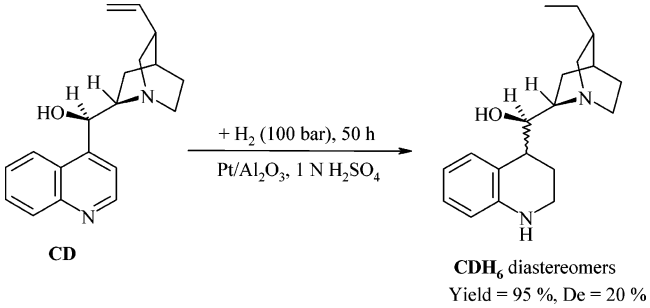

Figure 2. Scheme of hydrogenation of cinchonidine (CD) over Pt/Al_2O_3.

In the case of cinchonidine (CD), several conformers were identified and the population of the stable conformers could be estimated by NMR spectroscopy.[28,33,34] According to these results the most stable conformer of CD is the so-called "open (3)" conformer in which the N of the quinuclidine points away from the quinoline part and the O−H group is directed toward $H_{3'}$ (for atom labeling see Figure 1b). The presence of two "closed" conformers has also been demonstrated in solution by NMR and FTIR spectroscopies.[34] The population of different conformers could be correlated with the nature (dielectric constant) of the solvent.[34] It has also been shown that in acidic media (the quinuclidine N is protonated) the open (3) conformer is stabilized relative to the closed conformers due to the repulsion of the quinoline moiety.[35,36]

To the best of our knowledge, studies on the structure−property relation of hexahydrocinchona derivatives using an ab initio calculation and NMR results has not been published so far. Such a study is needed for the interpretation of the results obtained by the use of these compounds as a chiral source. Here we report the results of our theoretical study on the conformation of the two 1′,2′,3′,4′,10,11-hexahydrocinchonidine diastereomers (CDH_6) using ab initio method with a large basis set. The results of the calculations were compared with data obtained from NMR spectroscopy experiments.

2. Experimental Section

a. Materials. The preparation (see Figure 2) and identification of the two 1′,2′,3′,4′,10,11-hexahydrocinchonidine diastereomers (denoted as CDH_6-I and CDH_6-II) has been described recently.[27,37]

b. Methods. The ^1H, ^{13}C, and the 2D NMR spectra were recorded in benzene-d_6 (Aldrich, 99.6 at. % D) on a Bruker AVANCE DRX-500 (Karlsruhe, Germany) spectrometer operating at 500 MHz ^1H NMR frequency. The signal assignment was aided by 2D $^1H-^1H$ COSY and 2D $^1H-^{13}C$ heteronuclear correlation spectroscopy. The results of the nuclear Overhauser enhancement spectroscopy (NOESY) experiments were correlated with the computation data. Optical rotations were measured on a Polamat A (Carl Zeiss, Jena, Germany) polarimeter at 20 °C in ethanol (*c*, 1; *l*, 0.5); $[\alpha]_D$ values are given in deg cm^2 g^{-1}.

c. Calculations. The ab initio quantum chemical calculations were performed using GAUSSIAN 98 [38] on an Origin 2000 machine. Minimum-energy structures were computed by applying the B3LYP density functional hybrid method together with a 6-311G** basis set. X-ray diffractometry data published in the literature[39] were used as the initial structure for geometry optimization of CD. The molecule was fully relaxed. The optimized 4′-(*R*)- and 4′-(*S*)-1′,2′,3′,4′,10,11-hexahydrocinchonidines were obtained by adding the necessary H atoms in the corresponding orientation to the optimized CD and completely relaxing the structures. After obtaining the optimized structures, conformational searches were performed by rotation around the $C_{4'}-C_9$ (torsional angle τ_1: $C_{3'}-C_{4'}-C_9-C_8$) and C_9-C_8 (torsional angle τ_2: $C_{4'}-C_9-C_8-N_1$) bonds (see Figure 1) at an increment of 15°. Single-point energies of the resultant structures were calculated using the same functional and basis set.

3. Results and Discussion

Hydrogenation of CD over 5% Pt/Al_2O_3 in 1 N H_2SO_4 aqueous solution under 100 bar H_2 pressure after 50 h resulted in the formation of two 1′,2′,3′,4′,10,11-hexahydrocinchonidine diastereomers in over 95% isolated yield and 20% diastereomeric excess (see Figure 2).[27] These products contain a chiral center $C_{4'}$ formed during hydrogenation and a 1′,2′,3′,4′-tetrahydroquinoline ring system. Thus, beside rotation around the $C_{4'}-C_9$ and C_9-C_8 bonds, the mobility of the tetrahydroquinoline moiety can also lead to stable conformers of low energies.

a. Optimization of CD, 4′-(*R*)-CDH_6, and 4′-(*S*)-CDH_6. The optimized geometry of CD was identical with the open (3) conformer, obtained by Bürgi and Baiker,[34] as observed by comparing the values of the selected interproton distances and torsional angels (see Tables 1 and 2). The open (3) conformer of CD has the highest population in acidic solutions.[34−36] Accordingly, it was considered that during hydrogenations in acidic media CD mostly adopts this conformation.

Addition of hydrogen to $N_{1'}$, $C_{2'}$, $C_{3'}$, C_{10}, C_{11}, and $C_{4'}$ from the "pro-*R*" side of the optimized CD and relaxing the molecule led to an optimized geometry for 4′-(*R*)-CDH_6. This structure has the $H_{4'}$ atom in axial position; hence, it has been denoted as 4′-$(R)^{ax}$-CDH_6 (see Figure 3a). Because the tetrahydroquinoline moiety adopts a twisted conformation, the $C_{3'}$ atom can be positioned on either side of the plane of the aromatic ring. By

TABLE 1: Selected Interproton Distances (Å) for the Optimized Low-Energy Structures of CD and CDH_6 Diastereomers

	CD	4′-$(R)^{ax}$-CDH_6	4′-$(R)^{eq}$-CDH_6	4′-$(S)^{eq}$-CDH_6
$H_{5'} \leftrightarrow H_9$	2.12 (2.15)[a]	2.23	2.25	2.49
$H_{5'} \leftrightarrow H_8$	2.51 (2.46)[a]	4.53	3.74	4.34
$H_{5'} \leftrightarrow H_4$		3.31	2.64	2.53
$H_{5'} \leftrightarrow H_{6en}$	4.60 (4.78)[a]	4.06	4.66	4.84
$H_{4'} \leftrightarrow H_9$		3.00	2.40	2.35
$H_{4'} \leftrightarrow H_8$		3.34	3.67	2.38
$H_{4'} \leftrightarrow H_{3'ax}$		3.06	2.28	2.36
$H_{4'} \leftrightarrow H_{3'eq}$		2.47	2.63	2.58
$H_9 \leftrightarrow H_8$	2.51	2.45	2.57	2.59
$H_9 \leftrightarrow H_{6en}$	2.83	2.94	2.55	2.53
$H_9 \leftrightarrow H_{7en}$	4.13	3.68	3.61	3.61
$H_8 \leftrightarrow H_{3'ax}$	4.01 (4.00)[a]	2.48	4.28	3.61
$H_8 \leftrightarrow H_{3'eq}$		2.15	3.50	2.48
$H_{7ex} \leftrightarrow H_{3'eq}$	3.57	2.34	3.08	2.30

[a] Values in brackets are of open (3) conformer published by Bürgi and Baiker.[34]

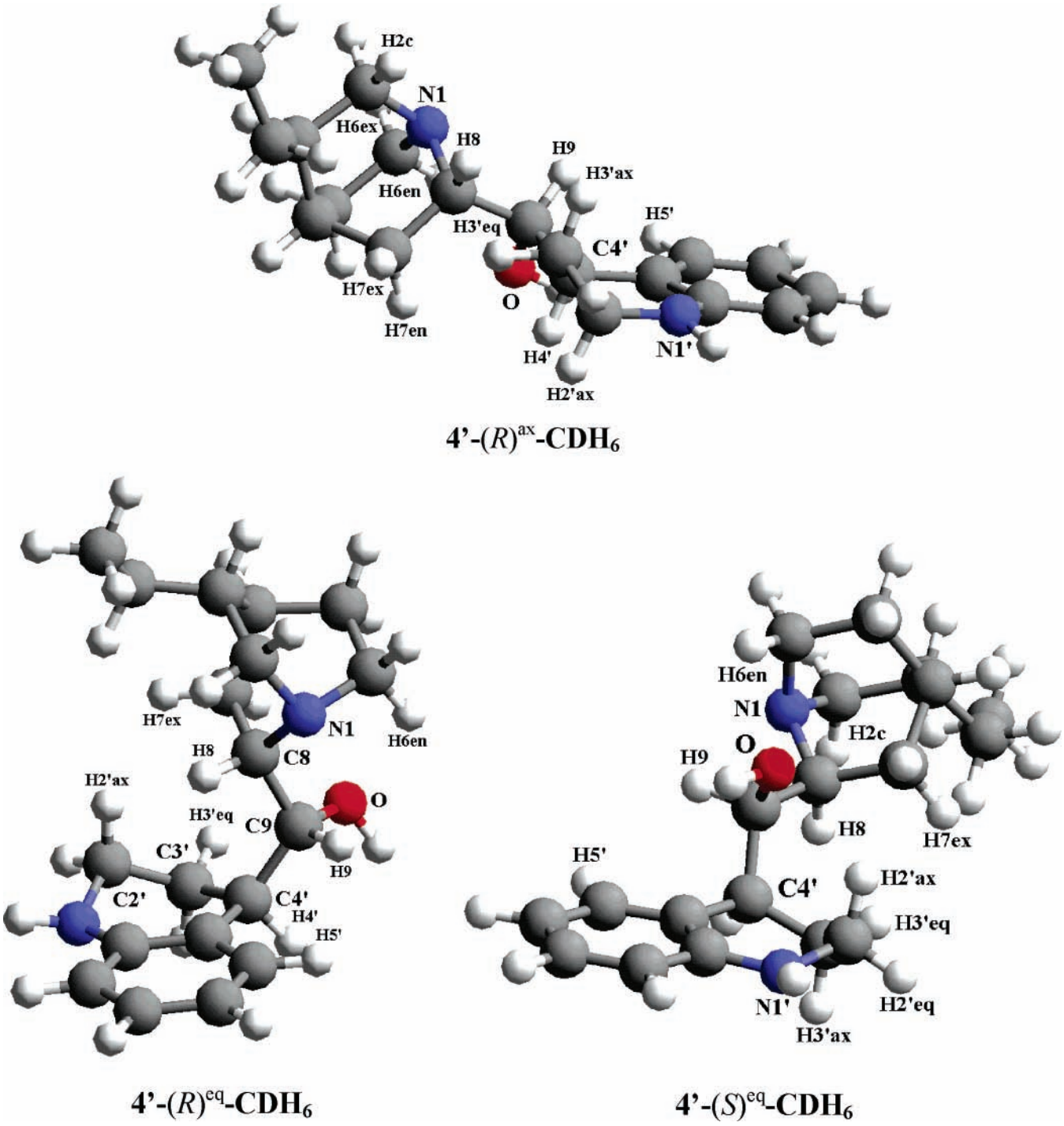

Figure 3. Ball and stick model of the optimized hexahydrocinchonidine structures: (a) 4′-$(R)^{ax}$-CDH_6; (b) 4′-$(R)^{eq}$-CDH_6; (c) 4′-$(S)^{eq}$-CDH_6.

TABLE 2: Selected Torsional Angles (deg) for the Optimized Low-Energy Structures of CD and CDH_6 Diastereomers

		CD	4′-$(R)^{ax}$-CDH_6	4′-$(R)^{eq}$-CDH_6	4′-$(S)^{eq}$-CDH_6
τ_1	$C_{3'}-C_{4'}-C_9-C_8$	99.6 (101.4)[a]	−29.9	65.1	56.3
τ_2	$C_{4'}-C_9-C_8-N_1$	154.0 (153.6)[a]	163.0	143.6	140.9
τ_3	$H_8-C_8-C_9-H_9$	−77.8 (−78.3)[a]	−70.0	−86.9	−87.8
	$C_{5'}-C_{9'}-C_{4'}-C_9$	−0.5	−19.0	−59.2	70.6
	$C_{9'}-C_{4'}-C_9-C_8$	−80.1	−156.8	−65.6	−177.4
	$H_{4'}-C_{4'}-C_9-H_9$		−154.1	−62.7	53.8
	$H_{4'}-C_{4'}-C_{3'}-H_{3'ax}$		−179.8	32.1	−44.2
	ΔE^b (kcal mol^{-1})		5.0	2.9	0

[a] Values in brackets are of open (3) conformer published by Bürgi and Baiker.[34] [b] Relative energies compared to the energy of the most stable 4′-$(S)^{eq}$-CDH_6 diastereomer.

moving the $C_{2'}$ and $C_{3'}$ atoms on the opposite side of the aromatic ring, as compared to their position in the optimized 4′-$(R)^{ax}$-CDH_6 and relaxing the molecule resulted in a low-energy conformer in which the $H_{4'}$ atom is positioned equato-

rially (see Figure 3b), denoted as 4′-(R)^{eq}-CDH$_6$. Adding the hydrogen to $C_{4'}$ from the "pro-*S*" side resulted in the optimized geometry with the $H_{4'}$ atom positioned equatorially (see Figure 3c), denoted as 4′-(S)^{eq}-CDH$_6$. However, moving the $C_{2'}$ and $C_{3'}$ atoms to the opposite sides of the aromatic ring plane, in a way similar to the case of the 4′-(R) diastereomer, led to a structure with axial $H_{4'}$ atom having significantly higher energy (more than 100 kcal mol^{-1}). Selected interproton distances, torsional angle values, and the relative energies of the obtained conformers are presented in Tables 1 and 2. For both the 4′-(S)- and 4′-(R)-diastereomers the conformers having equatorial $H_{4'}$ had lower energies. The quasi-equatorial position of $H_{4'}$ is clearly shown by the low $H_{5'} \leftrightarrow H_{4'}$ distances in these conformers (2.53 and 2.64 Å); in the case of the axial position this distance is increased (3.31 Å).

To define on which side of the aromatic plane the quinuclidine moiety is situated, the use of the $C_{5'}-C_{9'}-C_{4'}-C_9$ torsional angle is needed. This angle has negative values for the two 4′-(R) conformer and positive in the case of the 4′-(S) conformer. Accordingly, the quinuclidine moiety will be positioned on the opposite side of the tetrahydroquinoline system in the two diastereomers. The hexahydroderivatives adopt an "openlike" conformation, with the quinuclidine N_1 pointing away from the tetrahydroquinoline ring system (see Table 2, values of τ_1 and τ_2). However, the position of the hydroxyl group in the two low-energy structures, 4′-(R)^{eq}-CDH$_6$ and 4′-(S)^{eq}-CDH$_6$, is different. This difference may be of crucial importance in determining the accessibility and the binding direction of a reactant toward the hydroxyl group of these molecules.

b. Rotation around the $C_{4'}-C_9$ and C_9-C_8 Axis of the Hexahydrocinchonidines. In the case of CD rotation around the $C_{4'}-C_9$ and C_9-C_8 axis (variation of the τ_1 and τ_2 tosional angles) resulted in several conformers with close energies (within 2 kcal mol^{-1}) to that of the open (3) conformer.[34] Stepwise variation of torsional angles τ_1 and τ_2 and calculation of the corresponding single-point energies, for the three low-energy structures: 4′-(R)^{ax}-CDH$_6$, 4′-(R)^{eq}-CDH$_6$, and 4′-(S)^{eq}-CDH$_6$, resulted in the relative energy plots presented in Figure 4. It must be noted that the obtained structures were not fully optimized; thus, the obtained energies cannot be compared with the energies of the above-mentioned three structures. Our aim during this conformational search was to find structures corresponding to conformers possibly present in the solution of these compounds.

The obtained low-energy structures are presented in Figure 5 and selected interproton distances and torsional angle values are summarized in Tables 3 and 4, respectively.

A rotation of 90° around the $C_{4'}-C_9$ bond (change of τ_1) for 4′-(R)^{ax}-CDH$_6$ resulted in a low-energy structure denoted 4′-(R)^{ax}-CDH$_6^1$ (see Figure 5a). Decrease of the τ_2 torsional angle value also by about 90° resulted in the minimum denoted 4′-(R)^{ax}-CDH$_6^2$ (see Figure 5b). Stepwise modification of τ_1 or τ_2 torsional angles in the case of the other 4′-(R)-conformer (4′-(R)^{eq}-CDH$_6$) led to one structure having low energy denoted as 4′-(R)^{eq}-CDH$_6^1$ (see Figure 5c) and was obtained by decreasing the τ_1 value by about 90°. Application of the same procedure for the 4′-(S)^{eq}-CDH$_6$ diastereomer resulted in one low-energy structure by decreasing the torsional angle τ_2 value about 90°; the new structure was denoted as 4′-(S)^{eq}-CDH$_6^2$ (see Figure 5d).

One of the most important differences between the structures of the two diastereomers is the position of the quinuclidine moiety relative to the plane of the aromatic ring. This position is shown by the sign of the $C_{5'}-C_{9'}-C_{4'}-C_9$ torsional angle, which has negative values for all the low-energy structures in case of the 4′-(R)-diastereomer and positive values for the

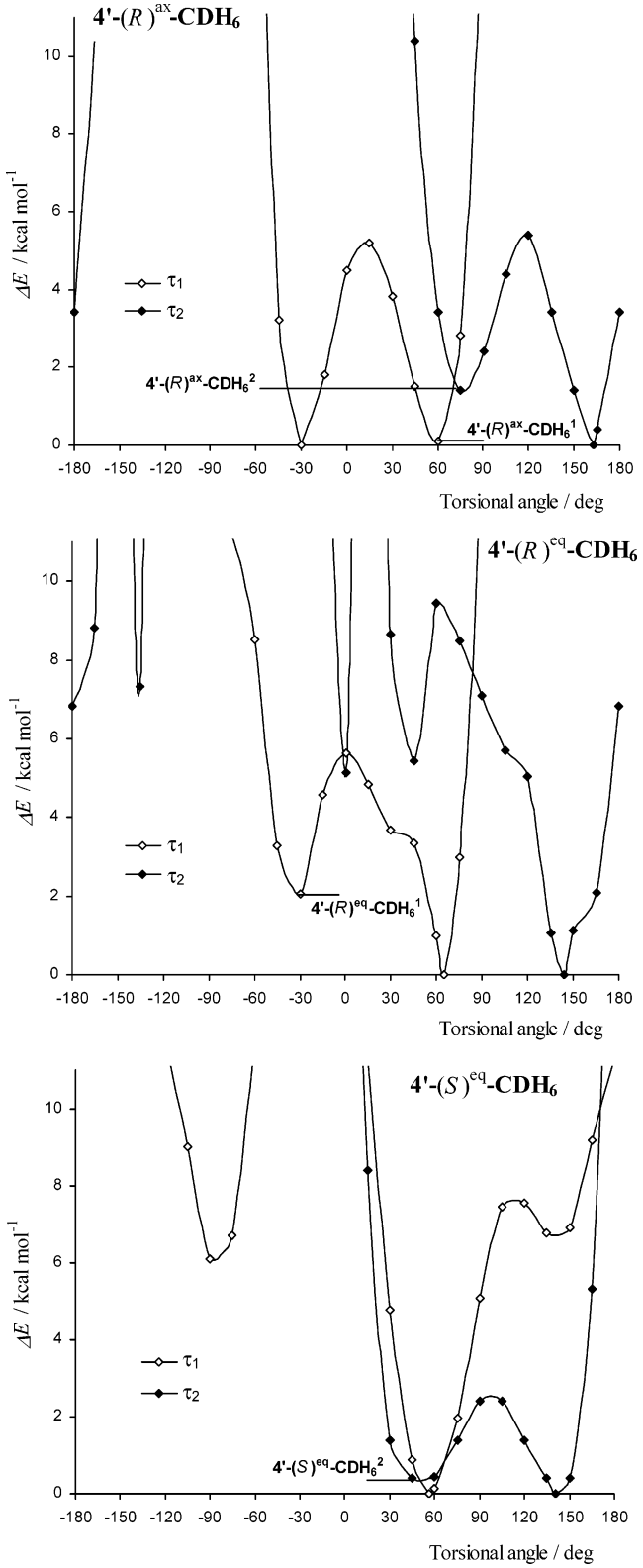

Figure 4. Relative single-point energy (ΔE) plots obtained by stepwise variation in 15° steps of torsional angles τ_1 and τ_2 and of (a) 4′-(R)^{ax}-CDH$_6$, (b) 4′-(R)^{eq}-CDH$_6$, and (c) 4′-(S)^{eq}-CDH$_6$.

structures of the 4′-(S)-diastereomer. Thus, irrespective of the axial or equatorial orientation of the $C_{4'}-C_9$ bond and the orientation of the N_1 atom or the hydroxyl group, the 4′-(R)-conformers have the quinuclidine moiety on the same side of the plane of the aromatic ring, while the 4′-(S)-conformers have it on the opposite side. It must be mentioned here that the 4′-

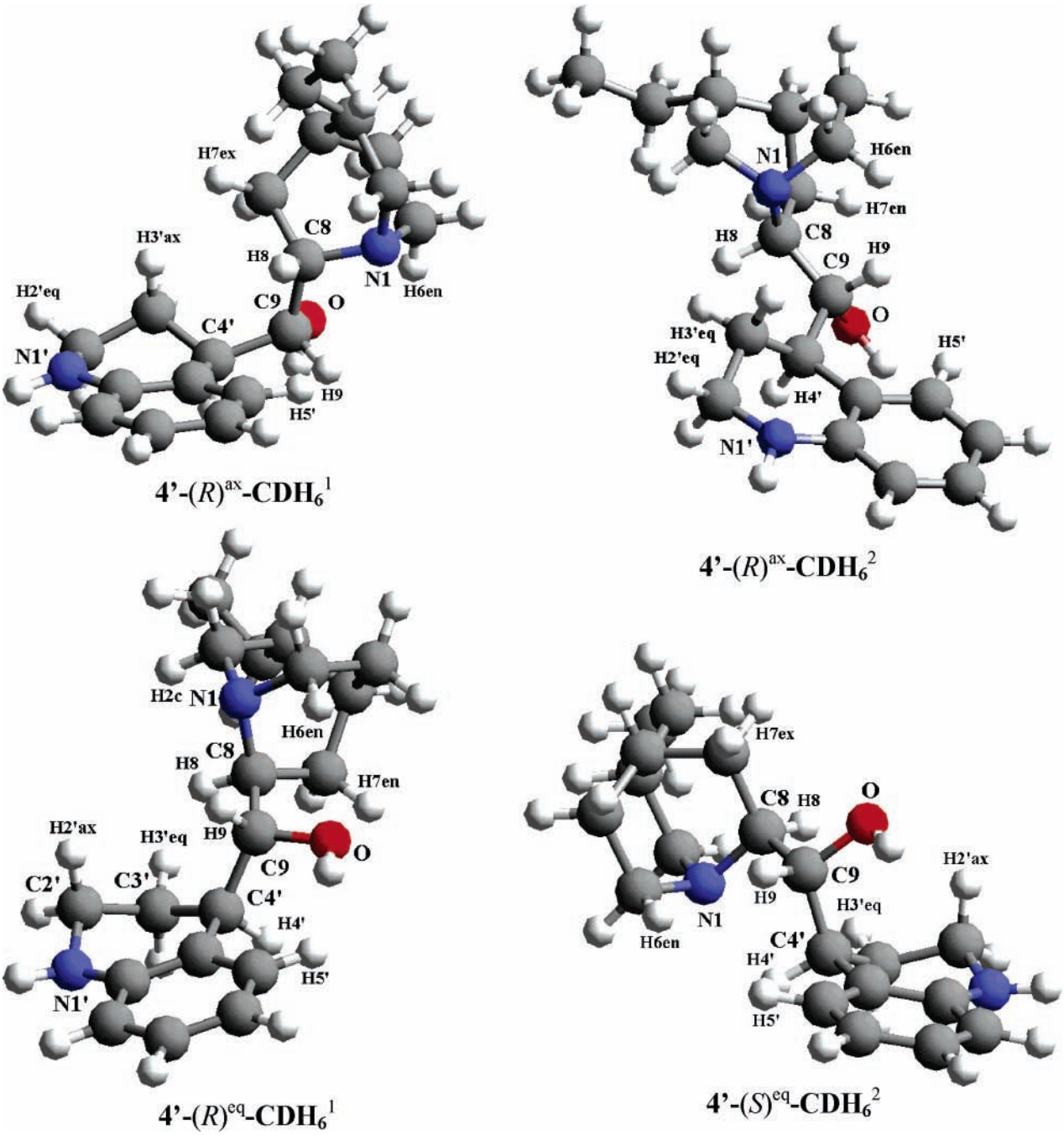

Figure 5. Ball and stick model of the low-energy structures obtained by stepwise variation in 15° steps of torsional angles τ_1 and τ_2 of the optimized conformers: (a) 4′-$(R)^{ax}$-$CDH_6{}^1$; (b) 4′-$(R)^{ax}$-$CDH_6{}^2$; (c) 4′-$(R)^{eq}$-$CDH_6{}^1$; and (d) 4′-$(S)^{eq}$-$CDH_6{}^2$.

(*R*)-conformers have the quinuclidine moiety on the same side as it is in the open (3) conformer of CD.

c. Comparison of the Results of the ab Initio Calculation with the NMR Data. ^{1}H NMR spectra and selected NOESY traces of the two isolated hexahydrocinchonidine diastereomers are presented in Figures 6 and 7. The assignment of the ^{1}H NMR signals for both diastereomers have been published recently (the two diastereomers were denoted according to their elution order, which has also been used in the present work).[27] The signal intensities in the NOESY traces were compared with the intensities of the $H_{5'}-H_{6'}$ cross-peaks (the $H_{5'} \leftrightarrow H_{6'}$ distance is 2.45 ± 0.02 Å, shown also by the calculation results). For a specified interprotonic distance the values for all the computed structures were taken into account and compared with the corresponding relative intensities of the NOESY cross-peaks from the traces of the two compounds.

Comparing the values obtained by calculation for the $H_{5'} \leftrightarrow H_9$ distance shows that, in all cases, except for 4′-$(R)^{eq}$-CDH_6,[1] this value is between 2 and 2.5 Å (see Tables 1 and 3). The only exception is the 4′-$(R)^{eq}$-$CDH_6{}^1$ conformer for which the said distance is 3.21 Å. On the other hand the intensity of the $H_{5'}-H_9$ cross-peak in the NOESY trace of the CDH_6-I diastereomer is very low, while in that of CDH_6-II has an intensity similar to the $H_{5'}-H_{6'}$ cross-peak (see Figures 6 and 7, traces b and d). Accordingly, one may assume that the configuration of the $C_{4'}$ chiral center in CDH_6-II diastereomer is *S*, in the CDH_6-I diastereomer is *R* and a conformer with a structure close to that of 4′-$(R)^{eq}$-$CDH_6{}^1$ is present in the solution of the 4′-(*R*)-diastereomer. Furthermore, the high values of the $H_{5'} \leftrightarrow H_8$ distance for all the computed structures (higher than 3.7 Å) except for the 4′-$(R)^{ax}$-$CDH_6{}^1$ conformer (2.37 Å) can also be correlated with the high-intensity $H_{5'}-H_8$ cross-peak observed

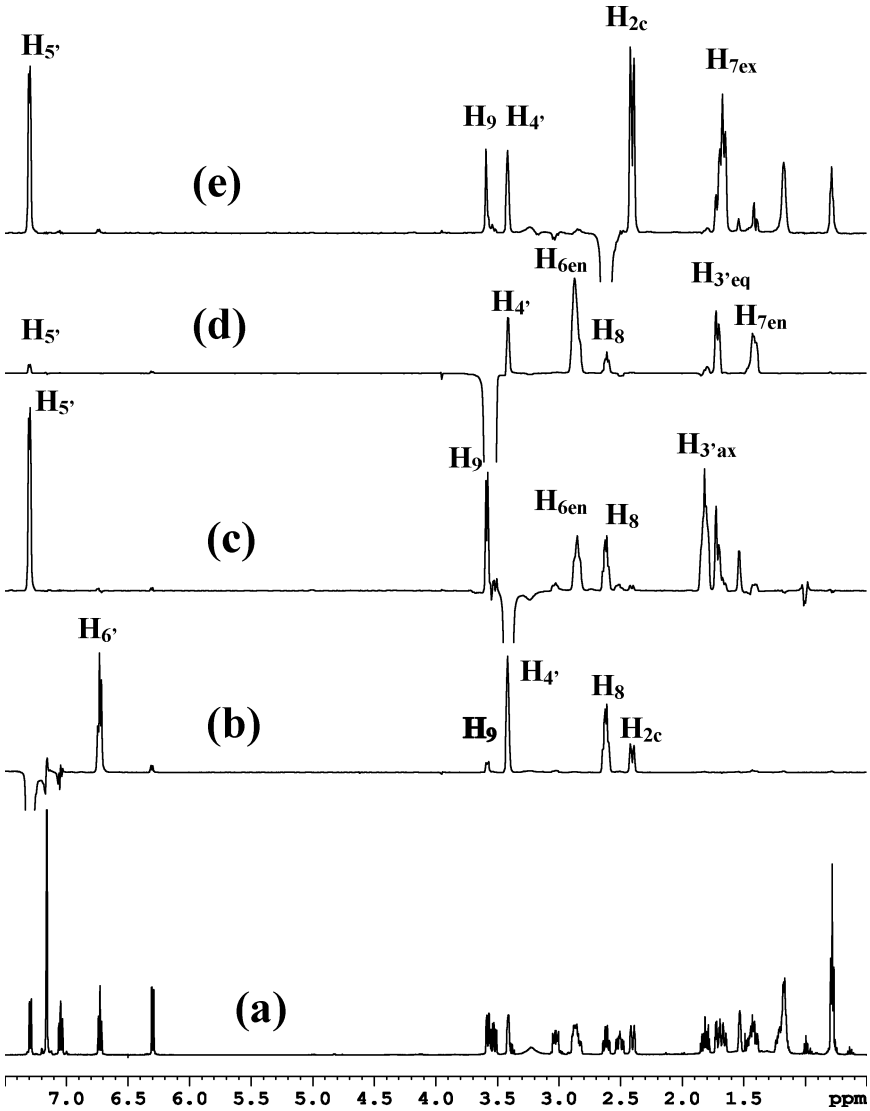

Figure 6. ^{1}H NMR spectrum and traces of the NOESY spectrum of CDH_6-I: (a) ^{1}H NMR spectrum and (b) $H_{5'}$, (c) $H_{4'}$, (d) H_9, and (e) H_8 NOESY traces.

TABLE 3: Selected Interproton Distances (Å) for the Low-Energy Structures Obtained by Variation of τ_1 or τ_2 Torsional Angles in a Step of 15°

	4′-(*R*)^{ax}-CDH_6^1	4′-(*R*)^{ax}-CDH_6^2	4′-(*R*)^{eq}-CDH_6^1	4′-(*S*)^{eq}-CDH_6^2
$H_{5'} \leftrightarrow H_9$	2.02	2.23	3.21	2.49
$H_{5'} \leftrightarrow H_8$	2.37	4.69	4.96	5.08
$H_{5'} \leftrightarrow H_4$	3.31	3.31	2.64	2.53
$H_{5'} \leftrightarrow H_{6en}$	4.64	4.00	4.50	3.04
$H_{4'} \leftrightarrow H_9$	2.46	3.00	2.98	2.35
$H_{4'} \leftrightarrow H_8$	3.72	2.73	3.15	3.23
$H_{4'} \leftrightarrow H_{3'ax}$	3.06	3.06	2.28	2.36
$H_{4'} \leftrightarrow H_{3'eq}$	2.47	2.47	2.63	2.58
$H_9 \leftrightarrow H_8$	2.45	2.97	2.57	3.01
$H_9 \leftrightarrow H_{6en}$	2.94	2.06	2.55	2.14
$H_9 \leftrightarrow H_{7en}$	3.68	2.80	3.61	2.49
$H_8 \leftrightarrow H_{3'ax}$	2.98	3.24	3.25	3.76
$H_8 \leftrightarrow H_{3'eq}$	3.98	2.11	1.59	2.16
$H_{7ex} \leftrightarrow H_{3'eq}$	3.29	4.44	3.05	4.47

in the NOESY trace of the CDH_6-I compound (see Figures 6 and 7, traces b and e). However, this also shows that this compound is present in solution (benzene) as a mixture of conformers.

The third distance which provided unambiguous evidence was the $H_{5'} \leftrightarrow H_{6en}$ distance, which had values above 4 Å except for the 4′-(*S*)^{eq}-CDH_6^2 structure (3.04 Å; see Tables 1 and 3). The $H_{5'}$ NOESY trace of CDH_6-I does not contain signal corresponding to H_{6en}. On the other hand the same trace of CDH_6-II presented a small signal of the H_{6en} proton which can be correlated only with the 3.04 Å distance measured in the 4′-(*S*)^{eq}-CDH_6^2 structure. Accordingly, one may assume that the CDH_6-II compound is the 4′-(*S*)-diastereomer. As was shown above, these compounds are present in solution as mixtures of conformers, making impossible the unambiguous interpretation of the other signals in their NOESY spectra.

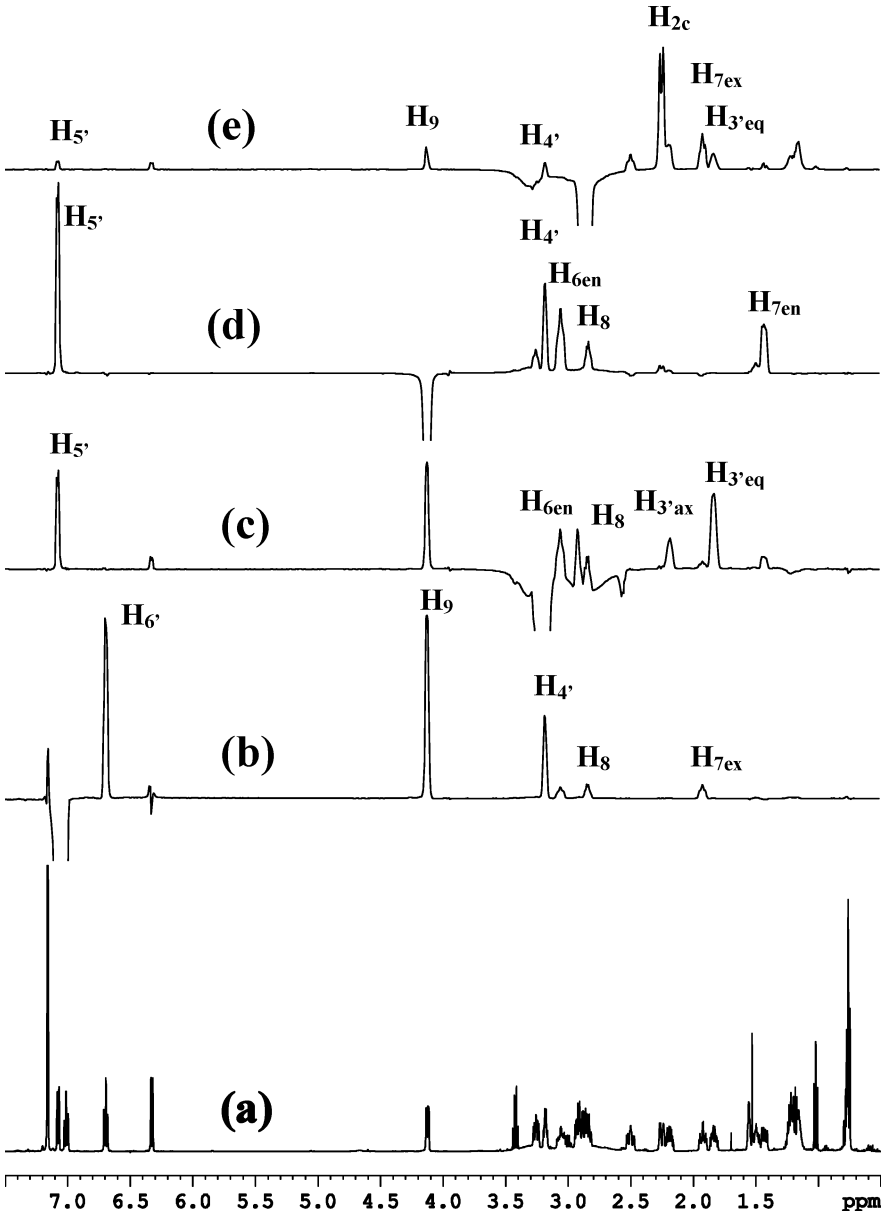

Figure 7. ^{1}H NMR spectrum and traces of the NOESY spectrum of CDH_6-II: (a) ^{1}H NMR spectrum and (b) $H_{5'}$, (c) $H_{4'}$, (d) H_9, and (e) H_8 NOESY traces.

TABLE 4: Selected Torsional Angles (deg) for the Low-Energy Structures Obtained by Variation of τ_1 or τ_2 Torsional Angles in a Step of 15°

		4′-(*R*)^{ax}-CDH_6^1	4′-(*R*)^{ax}-CDH_6^2	4′-(*R*)^{eq}-CDH_6^1	4′-(*S*)^{eq}-CDH_6^2
τ_1	$C_{3'}-C_{4'}-C_9-C_8$	60.0	−29.9	−30	56.3
τ_2	$C_{4'}-C_9-C_8-N_1$	163.0	75.0	143.6	45.0
τ_3	$H_8-C_8-C_9-H_9$	−70.0	−158.0	−86.9	176.3
	$C_{5'}-C_{9'}-C_{4'}-C_9$	−19.0	−19.0	−59.2	70.6
	$C_{9'}-C_{4'}-C_9-C_8$	−66.9	−156.8	−160.7	−177.4
	$H_{4'}-C_{4'}-C_9-H_9$	−64.1	−154.1	−157.8	53.8
	$H_{4'}-C_{4'}-C_{3'}-H_{3'ax}$	−179.8	−179.8	32.2	−44.2

In both ^{1}H NMR spectra the signals of H_9 protons appear as double doublets, coupled with the H_8 proton with coupling constants J_{H9-H8}, 8.7 Hz for CDH_6-I and 8.0 Hz for CDH_6-II, and with the $H_{4'}$ proton with coupling constants $J_{H9-H4'}$, 2.8 Hz for CDH_6-I and 3.9 Hz for CDH_6-II. Such high values of the J_{H9-H8} vicinal coupling constants can be obtained if these two H atoms are positioned close to staggered orientation. However, for both 4′-(*R*)- and 4′-(*S*)-diastereomers we have obtained such structures (4′-(*R*)^{ax}-CDH_6^2 and 4′-(*S*)^{eq}-CDH_6^2), having the $H_9-C_9-C_8-H_8$ torsional angle close to −180 and +180°, respectively (see Tables 2 and 4). Accordingly, the observed coupling constants cannot be used to support the conclusions drawn from the combined density functional theory (DFT) and NOESY data, as these coupling constants are dependent on the presence and the population of different conformers.

Identification of all the stable conformers of these two diastereomeric compounds needs further computational and experimental studies; a full conformational search may be the subject of our next study.

d. Comments on the Hydrogenation of CD and on the Behavior of the Hexahydroderivatives as Chiral Base Catalysts. As described above, the configuration of the $C_{4'}$ chiral

TABLE 5: Cinchona Derivatives and Results Obtained by Their Use as Base Catalysts in the Michael Addition of ECP to MVK

	configuration of the chiral center						results of the Michael addition[b]			
compound	C_3	C_4	C_8	C_9	$C_{4'}$	$[\alpha]_D^{20}$ [a]	reacn time (h)	yield (%)	$[\alpha]_D^{25}$ [c]	ee[d] (%)
CD	R	S	S	R		−108	8	90	−10.9	56
CDH_6-I	R	S	S	R	R	+117	24	12	−6.6	34
CDH_6-II	R	S	S	R	S	−56	24	76	+5.5	28

[a] Optical rotations of the cinchona derivatives (see Experimental Section). [b] Reaction conditions: 10 mmol ECP; 12 mmol MVK; 10 mL toluene; 0.02 mmol cinchona; 25 °C.[27] [c] Optical rotations of the isolated products (25 °C; *l*, 0.5 dm, neat). [d] Determined by chiral capillary GC.

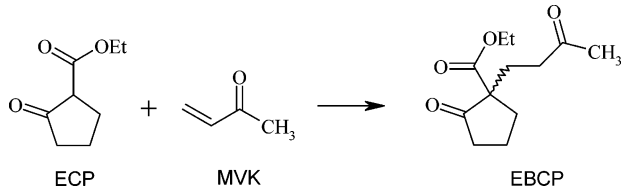

Figure 8. Base-catalyzed Michael addition of ECP to MVK.

center is *R* in CDH_6-I and *S* in CDH_6-II. Thus, the product mixture resulted in the hydrogenation of CD over Pt catalyst contains the 4′-(*S*)-diastereomer in excess (de = 20%). According to the computation results this diastereomer is more stable than the 4′-(*R*)-diastereomer. The 4′-(*S*)-conformers have lower electronic energies than the structures obtained for the 4′-(*R*)-diastereomer. This could be the reason of the formation in excess of the first one. The structures that resulted by calculation for the 4′-(*R*)-diastereomer have the quinuclidine moiety on the same side of the aromatic ring plane as in the open (3) conformer of CD. Thus, addition of H atoms from the metal surface to the open (3) conformer of CD and formation of the cis-addition product would lead exclusively to the 4′-(*R*)-diastereomer. The hydrogenation of CD resulted in the formation of both diastereomers;[27] moreover, according to the above identification the 4′-(*S*)-diastereomer was formed in excess. This may be the consequence of the presence of other CD conformers during the reaction.[34] Adsorption of the closed (1) conformer can lead by cis-addition of H_2 to the 4′-(*S*)-diastereomer. A more plausible explanation may be the tilted adsorption of CD on the Pt surface, demonstrated to take place at high CD concentrations.[40,41] The possible effect of the desorption and re-adsorption of tetrahydrocinchonidine intermediates also cannot be ruled out; the formation of such intermediates has been proven by electrospray ionization mass spectrometry.[26]

Finally, the configurational assignment of the two diastereomers allows us to comment on the surprising results reported recently, obtained by the use of these compounds as catalysts in base-catalyzed Michael addition.[27] Addition of ECP to MVK catalyzed by cinchona alkaloids resulted in the enantioselective formation of ethyl 1-(3′-oxobutyl)-2-oxocyclopentanecarboxylate (EBCP) (see Figure 8). Selected results obtained in this reaction together with the configuration of the chiral centers of the catalysts and their specific optical rotations are summarized in Table 5.

The ee obtained when either of the hexahydrocinchonidines were used as catalyst were lower than that obtained by the use of CD. However, the two diastereomers provided different enantiomers in excess. Thus, we can assume that one of the binding sites of the reactants during the reaction is present in the proximity of the new $C_{4'}$ chiral center of the alkaloid molecules. The use of the diastereomer assumed to be the 4′-(*R*)-isomer resulted in the excess product of the same configuration as that obtained by the use of CD. One may recall that the quinuclidine moiety in this diastereomer was positioned similarly as in CD, whereas in the 4′-(*S*)-diastereomer it was on the opposite side of the tetrahydroquinoline ring. Accordingly, it can be concluded that the relative orientation of the two ring systems in the catalyst molecule will play a crucial role in determining the way the substrates are bonded and will determine which enantiomer will form in excess. The low ee values obtained by using the hexahydroderivatives may be the consequence of the increased mobility of the quinuclidine moiety relative to the tetrahydroquinoline ring and consequently the decreased steric hindrances exerted on the substrates (as compared to CD). However, the presence of the $N_{1'}$ secondary nitrogen in the hydrogenated molecules makes possible further derivatization, by alkylation or acylation. Furthermore, this secondary amino group being relatively far from the stereogenic center of these molecules opens the possibility of using this functional group to bind these homogeneous chiral catalysts over solid supports, making them easily recyclable and reusable.

4. Conclusion

In summary we here performed an optimization by ab initio method using a large basis set for cinchonidine and its two 1′,2′,3′,4′,10,11-hexahydroderivatives. In the case of the two hexahydrodiastereomers the flexibility of the partially hydrogenated quinoline moiety was also taken into account, resulting in two low-energy structures for the 4′-(*R*) isomer. Our study included a conformational search on all the optimized geometries by independent incrementation of two torsional angles (τ_1 and τ_2) and calculating the single-point energies of the resulting structures. Thus, rotation around the $C_{4'}-C_9$ and C_9-C_8 bonds led to conformers of close energies, providing evidence on the possible presence of other stable conformers in the solution of these cinchonidine derivatives. We have compared our results with the data obtained from NOESY experiments. This comparison resulted in identification, within the limitation of this study, of the configuration of the $C_{4'}$ chiral center of the two isolated compounds, which was our primary goal. We could also propose a reason for the excess formation of a particular diastereomer, 4′-(*S*), which was more stable than all of the 4′-(*R*) conformers. The results obtained by the use of these CD derivatives as chiral catalysts in Michael addition of a cyclic β-keto ester to methyl vinyl ketone were interpreted on the basis of our identification. Our study is the first detailed study in this area aimed at elucidating a structure−property relationship for hydrogenated cinchonidine diastereoisomers.

Acknowledgment. Financial support by the Hungarian National Science Foundation (Grants OTKA TS 44690 and T 038342) is highly appreciated.

References and Notes

(1) Blaser, H.-U. *Chem. Rev.* **1992**, *92*, 935.
(2) Blaser, H. U.; Spindler, F.; Studer, M. *Appl. Catal., A* **2001**, *221*, 119.
(3) Kacprzak, K.; Gawroński, J. *Synthesis* **2001**, 961.
(4) Kolb, H. C.; VanNieuwenhze, M. S.; Sharpless, K. B. *Chem. Rev.* **1994**, *94*, 2483.

(5) Lygo, B.; Wainwright, P. G. *Tetrahedron* **1999**, *55*, 6289.
(6) Taggi, A. E.; Hafez, A. M.; Wack, H.; Young, B.; Drury, W. J., III; Lectka, T. *J. Am. Chem. Soc.* **2000**, *122*, 7831.
(7) Chen, Y.; Tian, S.-K.; Deng, L. *J. Am. Chem. Soc.* **2000**, *122*, 9542.
(8) Park, H.-G.; Jeong, B.-S.; Yoo, M.-S.; Park, M.-K.; Huh, H.; Jew, S.-S. *Tetrahedron Lett.* **2001**, *42*, 4645.
(9) Tye, H.; Comina, P. J. *J. Chem. Soc., Perkin Trans. 1* **2001**, 1729.
(10) Blaser, H. U.; Jalett, H. P.; Lottenbach, W.; Studer, M. *J. Am. Chem. Soc.* **2000**, *122*, 12675.
(11) Exner, C.; Pfaltz, A.; Studer, M.; Blaser, H.-U. *Adv. Synth. Catal.* **2003**, *345*, 1253.
(12) Hiemstra, H.; Wynberg, H. *J. Am. Chem. Soc.* **1981**, *103*, 417.
(13) Baiker, A. *J. Mol. Catal. A: Chem.* **1997**, *115*, 473.
(14) Pfaltz, A.; Heinz, T. *Top. Catal.* **1997**, *4*, 229.
(15) Baiker, A. In *Chiral Catalyst Immobilization and Recycling*; De Vos, D. E., Vankelecom, I. F. J., Jacobs, P. A., Eds.; Wiley-VCH: Weinheim, Germany, 2000; Chapter 7, pp 155−171.
(16) Bartók, M.; Felföldi, K.; Szöllösi, Gy.; Bartók, T. *Catal. Lett.* **1999**, *61*, 1.
(17) Szöllösi, Gy.; Bartók, M. *Chirality* **2001**, *13*, 614.
(18) Bartók, M.; Sutyinszki, M.; Felföldi, K.; Szöllösi, Gy. *Chem. Commun.* **2002**, 1130.
(19) Skita, A.; Brunner, W. *Ber. Dtsch. Chem. Ges.* **1916**, *49*, 1597.
(20) Jacobs, W. A.; Heidelberger, M. *J. Am. Chem. Soc.* **1922**, *44*, 1079.
(21) von Braun, J.; Lemke, G. *Justus Liebigs Ann. Chem.* **1930**, *478*, 176.
(22) Suszko, J.; Golankiewicz, B. *Rocz. Chem.* **1968**, *42*, 477.
(23) Niwa, S.; Imai, S.; Orito, Y. *J. Chem. Soc. Jpn.* **1979**, 1118.
(24) Niwa, S.; Imai, S.; Orito, Y. *J. Chem. Soc. Jpn.* **1980**, 670.
(25) Morawsky, V.; Prüsse, U.; Witte, L.; Vorlop, K.-D. *Catal. Commun.* **2000**, *1*, 15.
(26) Bartók, M.; Szöllösi, Gy.; Balázsik, K.; Bartók, T. *J. Mol. Catal. A: Chem.* **2002**, *177*, 299.
(27) Szöllösi, Gy.; Forgó, P.; Bartók, M. *Chirality* **2003**, *15*, S82.
(28) Aune, M.; Gogoll, A.; Matsson, O. *J. Org. Chem.* **1995**, *60*, 1356.
(29) Dijkstra, G. D. H.; Kellogg, R. M.; Wynberg, H. *Recl. Trav. Chim. Pays-Bas* **1989**, *108*, 195.
(30) Dijkstra, G. D. H.; Kellogg, R. M.; Wynberg, H.; Svendsen, J. S.; Marko, I.; Sharpless, K. B. *J. Am. Chem. Soc.* **1989**, *111*, 8069.
(31) Dijkstra, G. D. H.; Kellogg, R. M.; Wynberg, H. *J. Org. Chem.* **1990**, *55*, 6121.
(32) Carroll, F. I.; Abraham, P.; Gaetano, K.; Mascarella, S. W.; Wohl, R. A.; Lind, J.; Petzoldt, K. *J. Chem. Soc., Perkin Trans. 1* **1991**, 3017.
(33) Berg, U.; Aune, M.; Matsson, O. *Tetrahedron Lett.* **1995**, *36*, 2137.
(34) Bürgi, T.; Baiker, A. *J. Am. Chem. Soc.* **1998**, *120*, 12920.
(35) Ferri, D.; Bürgi, T.; Baiker, A. *J. Chem. Soc., Perkin Trans. 2* **1999**, 1305.
(36) Bürgi, T.; Vargas, A.; Baiker, A. *J. Chem. Soc., Perkin Trans. 2* **2002**, 1596.
(37) Bartók, T.; Szöllösi, Gy.; Felföldi, K.; Bartók, M.; Thiel, J. *J. Mass Spectrom.* **2000**, *35*, 711.
(38) Frisch, M. J.; Trucks, G. W.; Schlegel, H. B.; Scuseria, G. E.; Robb, M. A.; Cheeseman, J. R.; Zakrzewski, V. G.; Montgomery, J. A.; Stratmann, R. E.; Burant, J. C.; Dapprich, S.; Millam, J. M.; Daniels, A. D.; Kudin, K. N.; Strain, M. C.; Farkas, O.; Tomasi, J.; Barone, V.; Cossi, M.; Cammi, R.; Mennucci, B.; Pomelli, C.; Adamo, C.; Clifford, S.; Ochterski, J.; Petersson, G. A.; Ayala, P. Y.; Cui, Q.; Morokuma, K.; Malick, D. K.; Rabuck, A. D.; Raghavachari, K.; Foresman, J. B.; Cioslowski, J.; Ortiz, J. V.; Stefanov, B. B.; Liu, G.; Liashenko, A.; Pislorz, P.; Komaromi, I.; Gomperts, R.; Martin, R. L.; Fox, D. J.; Keith, T.; Al-Laham, M. A.; Peng, C. Y.; Nanyakkara, A.; Gonzalez, C.; Challacombe, M.; Gill, P. M. W.; Johnson, B. G.; Chen, W.; Wong, M. W.; Andres, I. L.; Head-Gordon, M.; Replogle, E. S.; Pople, J. A. *Gaussian 98*, Revision A.9; Gaussian, Inc.: Pittsburgh, PA, 1998.
(39) Oleksyn, B. J. *Acta Crystallogr.* **1982**, *B38*, 1832.
(40) Ferri, D.; Bürgi, T. *J. Am. Chem. Soc.* **2001**, *123*, 12074.
(41) Ferri, D.; Bürgi, T.; Baiker, A. *J. Catal.* **2002**, *210*, 160.